Design for a low-cost, geosynchronous, 2.4-meter UV/EUV Solar System Observatory

Bernhard Haisch[a], Paul Robb[a], Keith Strong[a] and Donald Shemansky[b]

[a]Lockheed Martin Advanced Technology Center, 3251 Hanover Street, Palo Alto, CA 94304-1191
[b]Department of Aerospace Engineering, University of Southern California, Los Angeles, CA 90089

ABSTRACT

Studies were initiated in 1995 at the Lockheed Martin Advanced Technology Center in Palo Alto to explore both the application of new technologies and the economical utilization of commercial products to the design of a new generation of scientific research satellites. A 2.4-meter Solar System Observatory (SSO) has been designed to carry out as its primary mission imaging and spectroscopy of comets and of the outer planets from geosynchronous orbit. Such a Hubble-class telescope with a science payload consisting of four UV/EUV spectrographs and a high-resolution imager having 0.06 arcsec spatial resolution can now be built and launched within the budget of a NASA Discovery Mission. Following a one-year science program under the direction of the principal investigator, the SSO would transition to a guest observer facility. Although optimized for cometary and planetary measurements, SSO would have outstanding capability for a variety of astrophysical measurements. SSO would also serve as a prototype for other similar low-cost space observatories that could be optimized for stellar, extragalactic and other applications.

Keywords: Discovery Mission, solar system, planets, comets, telescope, observatory, ultraviolet

1. INTRODUCTION

The Solar System Observatory (SSO) is designed to be a NASA Discovery Mission consisting of a lightweight 2.4-m telescope in geosynchronous orbit with a scientific instrument package comprising four spectrographs and a high-resolution electronic camera. The spectrographs are designed to operate in the UV/EUV (55–320 nm) with a spectral resolution in the range of $\lambda/\Delta\lambda$ of 200 to 20000 and a spatial resolution of 0.18 arcsec over a 200 arcsec slit. The broadband UV imaging camera will produce images having a diameter of 0.06 arcsec. The telescope design and mirror surface have been carefully optimized to provide off-axis light rejection up to a factor of 1400 better than the Hubble Space Telescope (HST). An inertial angle sensor (IAS) provides an optical reference that is stable in inertial space. This permits us to control the line of sight through articulating the secondary mirror in tip-tilt, stabilizing the image to 0.005 arcsec without imposing costly requirements on the spacecraft attitude control system.

The 1145-kg observatory will be launched on a Delta 7920 into a 28.5-deg geosynchronous orbit over the Pacific. This orbit provides 24-hour observing, minimal interference from terrestrial emissions, and simplified mission operation. It also avoids the South Atlantic radiation anomaly that has plagued the International Ultraviolet Explorer (IUE) and HST. Mission lifetime is 5 to 7 years. The spacecraft will be derived from Lockheed Martin's LM-900 standard bus, providing attitude control, power, communications, and command and data handling with minimal modifications. Studies at the Lockheed Martin Advanced Technology Center that have been ongoing since 1995 indicate that, thanks to application of new technologies and the economical utilization of commercial products, such a major observatory can be built and launched within the cost and weight constraints of the Discovery Mission program. The telescope, instrument, spacecraft, and third stage are shown in the Delta 7920 10L launch fairing in Figure 1. Note that the secondary mirror support structure had to be modified to fit within the available length.

2. MISSION CONSTRAINTS

Based on the draft Announcement of Opportunity issued by NASA on January 30, 1998, key technical and cost constraints for a Discovery Mission are:

B.H: Email: haisch@starspot.com; Telephone: 650-424-3268; Fax: 650-424-3994
P.R.: Email: paul.robb@lmco.com; Telephone: 650-424-3309; Fax: 650-354-5002
K.S.: Email: keith.strong@lmco.com; Telephone: 650-354-5136; Fax: 650-424-3994
D.S.: Email: dons@athena.usc.edu; Telephone: 213-740-7184; Fax: 213-740-7774

Part of the SPIE Conference on Space Telescopes and Instruments V • Kona, Hawaii • March 1998
SPIE Vol. 3356 • 0277-786X/98/$10.00

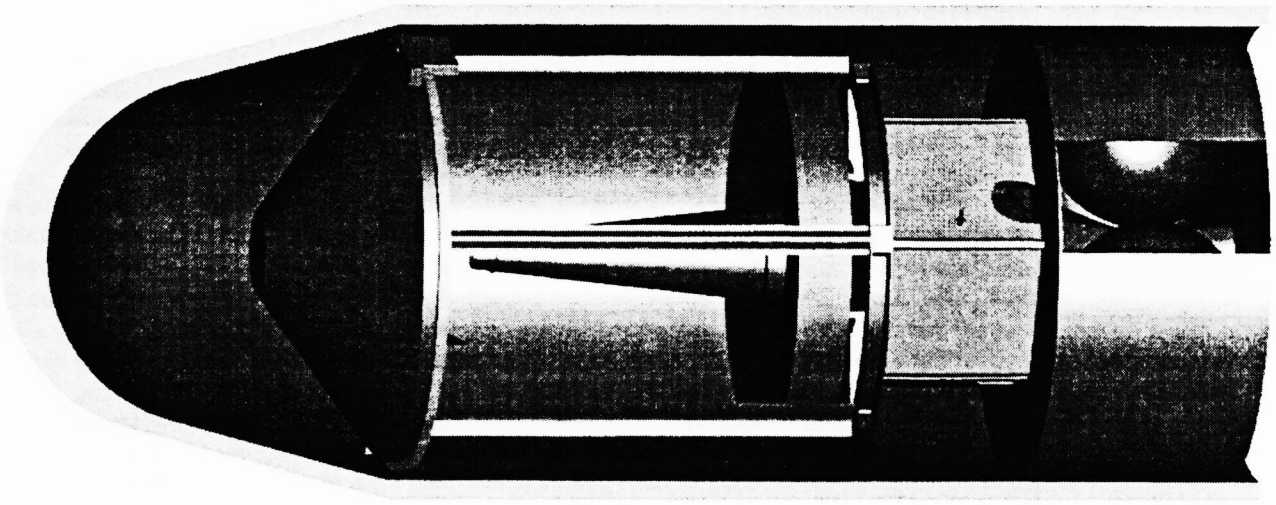

Figure 1. View of the 2.4-m Solar System Observatory (SSO) in Launch Fairing

- Phase A/B and C/D (launch plus 30 days) cost together not to exceed $209M (FY 1999 dollars).
- Launch to take place no later than Sept. 30, 2004. This is approximately 5 years after down selection. However, phase C/D is not to exceed 36 months.
- Use of a Delta II 7920-7925 (or smaller) expendable launch vehicle (provided at no cost).

Location in a geosynchronous orbit has three major advantages. Long, unocculted observations become possible. Sudden thermal gradients on the satellite and instruments are avoided. A dedicated ground facility (staffed by both undergraduate and graduate students) located on the University of Southern California (USC) campus can maintain continuous contact with the spacecraft, thus supporting real-time interactive observing capabilities for scientists (and invaluable training for students). For 24-hour orbits, the throw weight of a Delta II 7920 with a liquid bipropellant upper stage translates into the launch weight capabilities shown in Table 1.

From the latitude of USC (34 deg N), a 28.5-deg-inclination orbit with an eccentricity of up to 0.2 would be acceptable, provided that the longitude is within 30 deg of 115 deg W. This translates into a maximum launch weight of 1473 kg.

The work space of the Delta 7920 10L launch fairing is sufficient for the 2.4-m telescope, spacecraft bus, and liquid-bipropellant third stage, although the telescope secondary mirror support structure will be modified to fit within the available envelope.

3. SOLAR SYSTEM SCIENCE OBJECTIVES

The SSO was designed to complement the capabilities of the HST for observation of planets and comets in our solar system in four areas.

- The SSO spectrographs are designed to operate at shorter wavelengths (55–320 nm) than HST, since this is the prime region for emission and absorption from comets and planetary atmospheres.
- Scattered light is greatly reduced by a combination of Gregorian optics, baffles, field stops and low mirror surface roughness (5–10 Å rms in comparison to 36 Å rms for the HST primary).

Table 1. Launch Weight of Delta II 7920 in Kilograms, for Various Inclinations and Eccentricities

Inclination	Eccentricity			
	0.0	0.1	0.2	0.5
5-deg	1183	1233	1288	1468
28.5-deg	1288	1333	1473	1573

- Observations as close as 7 deg to the Sun are possible (the HST limit is 50 deg).
- Geosynchronous orbit enables long, unocculted observations without geocoronal interference.

With such a facility, substantial progress can be made in our understanding of the origin and evolution of the solar system. A key advance is the ability to observe comets near perihelion. It is also important to be able to detect and measure weak emissions in the presence of bright off-axis objects, e.g., within a few tens of arcsec above planetary disks. The scattered light rejection of SSO ranges up to 1,400 times that of HST, for 5 Å SSO mirror surfaces, depending on the off-axis angle.

Cometary science will benefit from the ability of the SSO to measure atomic and molecular abundances in the nucleus. The composition of ices in cometary nuclei provide insight into the temperature and density variations in the outer protoplanetary disk.[1] Key species sensitive to formation temperatures are the molecules of CO and CO_2 and the noble gases Ne, Ar, and Kr.[2] All of these are best observed in the ultraviolet. The 0.06-arcsec spatial resolution of the SSO will allow us to probe the S_2 emission, which is typically only detectable within a few hundred kilometers of the nucleus. The long spectrograph slit (200 arcsec) will allow us to determine the spatial profile of, for example, H_2O, out to distances from the nucleus that are large compared to plausible production and excitation scale-lengths. We can address the question of heterogeneity within individual cometary nuclei, observing whether the nucleus is composed of several cometesimals via rotational modulation measurements made possible by the uninterrupted target visibility from geosynchronous orbit. Sublimation behavior can also measured from the continuous monitoring that is possible. Atomic compositions can be determined from H, C, O, S, and N. A physically significant classification scheme for comets based on physical parameters has recently begun to be developed, but it is severely limited by our ability to observe comets from the ground.[3] A key goal of the SSO is to understand comet evolution by separating primordial abundance from evolutionary processes. Systematic comparative studies of many comets, each observed over a range of heliocentric distances, become possible over the lifetime of this observatory.

The Io Plasma Torus (IPT) is composed primarily of O^+, O^{++}, S^+, S^{++}, and S^{+++} supplied by the volcanoes on Io. The ion and electron temperatures are radically different ($T_i \sim 60$ eV, $T_e \sim 5$ eV), and even after two decades of observation we have an incomplete understanding of the energy input: the optically thin radiative losses are known but at least half the energy input is unaccounted for.[4,5] The SSO spectrographs will have a spatial resolution of 6 pixels across Io, and the length of the slit spans the IPT. Auroral activity in the SO_2 atmosphere of Io can be probed. Key emission lines to be observed are O II 53.9 nm and 83.4 nm, O III 70.3 nm, Si III 68.0 nm, 82.5 nm, and 101.8 nm, and Si IV 107.0 nm. The small-scale structure of the IPT is known to be highly variable; the vertical distribution and longitudinal variation of emissions in these ions will probe the composition and the electron and ion temperatures of the IPT. The SSO can observe the outward radial diffusion of the iogenic ions versus the inward diffusion/convection of more energetic ions from the outer magnetosphere.

The magnetospheres and thermospheres of Jupiter and Saturn will be the focus of several studies. There are major differences between these two planets. In contrast to the IPT-dominated magnetosphere of Jupiter, Saturn's is dominated by neutral gas.[6,7] There is a highly variable OH population in the Saturn magnetosphere that is three orders of magnitude more dense than had been expected from theoretical considerations. It is essential to obtain a detailed map of the Saturn magnetosphere. A key SSO strength (over the HST) will be the ability to reject off-axis scattering, which limits HST/STIS to measurements beyond three Saturn radii. The SSO will allow mapping the magnetospheric OH down into the ring region. We will also search for neutral oxygen. The thermospheres of the outer planets are greatly expanded and an order of magnitude hotter than had been expected.[8] Moreover, there is no correlation with distance from the Sun. A substantial heating mechanism must be operating, such as energy input from auroral precipitation, gravity wave heating, or soft particle precipitation.

The H_2 Rydberg bands show airglow in the outer planets, as observed by Voyager, the Hopkins Ultraviolet Telescope, and Galileo. The SSO will be ideal for the very long exposures necessary, for example, for determining the H_2 dayglow rotational temperature on Jupiter. It should be possible to determine the thermospheric temperature as a function of local time on Jupiter and Saturn. Lyman-alpha and higher series members can be measured; the cause of the mysterious Lyman-alpha bulge in the Jovian dayglow may be discovered thanks to the ability to map it systematically as a function of local time and system III longitude.[9] We will also map the He 58.4-nm Jovian dayglow. The photochemistry of Jupiter's middle and upper atmosphere will be studied by mapping NH_3, C_2H_2, C_2H_4, and C_2H_2. The Jovian aurora varies on time scales ranging from seconds to decades. Long term monitoring will be carried out and examined against such variables as local time, magnetic longitude, and solar activity. The SSO camera will provide context images of Jupiter.

These are simply the top-level highlights of an extensive comet and outer planet science program to be carried out during the first year of operation.

4. OTHER ASTROPHYSICAL CAPABILITIES

Although designed to be optimized for observations of planets and comets within our solar system, the SSO is a very capable instrument for numerous astrophysical research programs. Key characteristics in comparison to the HST and the long-lived (1978-1996) IUE are instructive.

- This facility would have the powerful combination of IUE-like dwell times and spectral resolution with HST-like light-gathering power (240-cm versus 45-cm aperture, a factor of 28 in collecting area).
- Long, uninterrupted dwell times from geosynchronous orbit are possible for studying eclipsing binaries, flares, mass loss and mass accretion, and rotational modulation of activity.
- Flexible scheduling of time variable objects is permitted; e.g., synoptic monitoring of active galactic nuclei, variable stars, and eclipsing binary stars is possible. This flexibility also enhances multiwavelength coordinated observing capability: Observing plans can change in real time based on incoming data or the situation at other coordinated sites.
- Rapid response to targets of opportunity is feasible, e.g., novae and supernovae.
- Spectral mapping of extended astronomical sources can be carried out with the 200 arcsec slit, e.g., galaxies, stellar and extragalactic jets, and planetary nebulae.
- Given its lower cost, the SSO is more likely to be used in a "discovery mode" to simply search for new phenomena.

While the 550–912 Å region would be of no use for extra-solar-system observations, due to the opacity of the interstellar medium as verified by the Extreme Ultraviolet Explorer, with a spectral resolution of up to $\lambda/\Delta\lambda = 20{,}000$ (in comparison to the IUE Echelle spectrographs having $\lambda/\Delta\lambda = 12{,}000$–$13{,}000$) a variety of opportunities arise in the area of solar-stellar astrophysics in the 912-3200 Å region.[10] In many stars, it will be possible to measure the redshifting of emission lines formed at temperatures of T=15,000–20,000 K indicating plasma downflows in (presumably) magnetic loops at these temperatures, a phenomenon discovered in IUE spectra[11] similar to that observed in the solar spectrum above active and quiet regions.[12]

Mass ejections associated with stellar flares could be witnessed; these involve velocities of 1000 km/s or more. We could explore the characteristics of chromospheres and winds across the Hertzsprung-Russell diagram to understand the relationship between the evolution of internal stellar structure and magnetic dynamo, and the external extended atmosphere with its magnetic loop structures. Does the basic dynamo mode change? Does magnetic braking work the same for all stars of a given mass?

Stellar surface mapping becomes possible. Techniques have been devised to deconvolve emission line profiles to identify the passage of individual outer atmospheric structures across the surface as the star rotates. This allows us to investigate compact atmospheric structures on scales small compared to the stellar radius.

For a long-lived mission, stellar cycles could be observed. The Maunder Minimum in solar activity from about 1640 to 1715 AD generated a "Little Ice Age" during which glaciers grew in the Alps, Baltic seaports were frozen over in the winter longer than today, and growing seasons were shorter. Baliunas and Jastrow[13] studied 74 solar-like stars and found suggestive evidence of a bimodal distribution in surface coverage of solar-like plage. By extending this and by monitoring stellar cycles we may be able to gather valuable insight into the likely temporal variations of the Sun from a "snapshot" of the present activity states of solar twins.

Mass flows in binaries and hot winds in early-type stars also present excellent opportunities. Multiple gas streaming episodes have been observed in the Algol-type binary U Cep (B7-8V+G8III-IV) in which optically thick plasma from the evolved G star appears to engulf the B companion. At the upper end of the main sequence, hot winds occur in hundreds of OB stars. We would do large-scale sampling to determine wind properties as function of spectral type and metallicity (since the winds are radiatively driven, hence strongly dependent on opacity), with repeat observations to investigate variability. Note also that terminal velocities and mass loss rates are different in the LMC, SMC, M31, and M33 than for stars in our Galaxy. SSO could sample more stars in more distant galaxies. We could study how the winds change as stars evolve. Mass loss rates may increase by 100–1000 from the upper main sequence to the hydrogen-burning shell stage to Wolf-Rayet stars...but there is very little change in luminosity. What causes such massive increase in radiatively (opacity) driven winds? Winds in the central stars of planetary nebulae and the planetary nebulae themselves are also good targets.

In the area of extragalactic research, consider the following two examples of long-term monitoring and large sample surveying carried out by the IUE. Thanks to 45 days of continuous monitoring of the Seyfert I galaxy NGC 7469, statistically significant

evidence was found for the existence of time delays between continuum variations in different parts of the spectrum. Owing to a large sample survey, the spectra of individual low-luminosity active galaxies has shown that, in the UV, two different classes can be identified, representing physically different objects, one group characterized by emission lines and the other group by absorption lines. The place of these two classes in the context of the general unified theories of active galaxies is unclear.

5. THE TELESCOPE AND INSTRUMENT PACKAGE

For suppression of stray light, a Gregorian telescope design is superior to a Cassegrain system. There is a slight penalty in extra length, but this amounts to only about 0.5 m. The focal surface is also more steeply curved. This does not pose a problem for the SSO instruments. The 2.4-m-diameter primary mirror is f/1.15, and the telescope focal ratio is f/20.0. Field and Lyot stops are placed at the internal focus and exit pupil respectively to suppress secondary scatter. The Gregorian designs gain in stray light rejection over a Cassegrain is approximately a factor of 20 to 10,000 (for equivalent mirror surface roughnesses), depending on the off-axis angle. The design is shown on Figure 2. The prescription is included at the end of this paper.

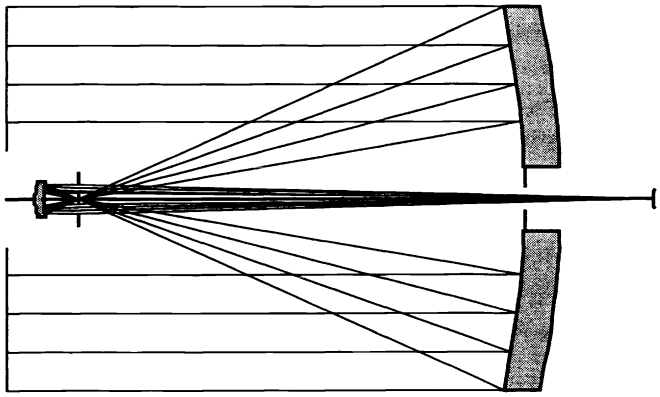

Figure 2. SSO Gregorian Telescope

The near-UV imager, operating over the 250–450 nm spectral band, is a flight spare Cassini camera used with minimum modifications.

Each spectrograph consists of a slit at the Gregorian focus followed by a grating formed on a concave toroid.

The focal plane layout is shown on Figure 3. The center of the field, measuring 0.076 deg square (approximately 64 mm), is used by the near-UV imager. Slits for the spectrographs are placed at four locations around the edge of the visible imager, 0.058 deg from the optical axis.

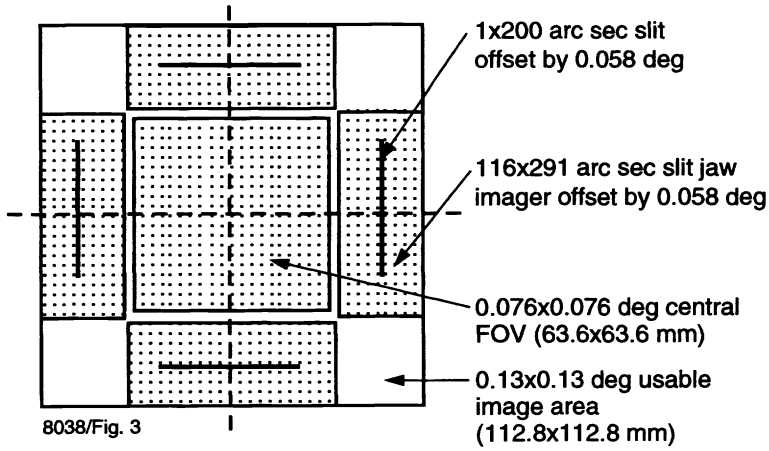

Figure 3. Focal Plane Layout

The polychromatic diffraction point spread function (PSF) for the telescope was calculated for the 250–450 nm spectral region. The Strehl ratio is 1.0 on axis and 0.86 at the edge of the UV imager's field of view. The two PSFs are shown in Figure 4.

The ULE (ultralow-expansion fused silica) primary mirror is of meniscus construction with lightweighting cavities and closed back. It is lightweighted by 97 percent, and weighs 159 kg, for an aerial density of 35 kg per square meter. Grinding and polishing such a lightweight mirror has been made possible by the technological advances in recent years (much of this funded by SDI) in computer-controlled small tool polishing combined with ion figuring to remove residual print-through. A mirror blank identical in size, curvature, and weight to the SSO mirror has been built as a technology demonstrator, and may be available as a backup mirror should one be required. A section of this mirror, 55 cm in diameter, has been ground, polished, and tested, proving the feasibility of this lightweight structure.

A bulkhead made of graphite epoxy (GrE) forms the central structural member for the SSO, as shown on Figure 1. To this bulkhead is attached the telescope primary mirror and metering tube, the instruments, and the spacecraft bus. The metering tube is an aluminum monocoque structure with stiffening rings and GrE metering rods held in four channels spaced equally around the perimeter. The secondary mirror assembly is attached to the metering tube through flexures that provide the

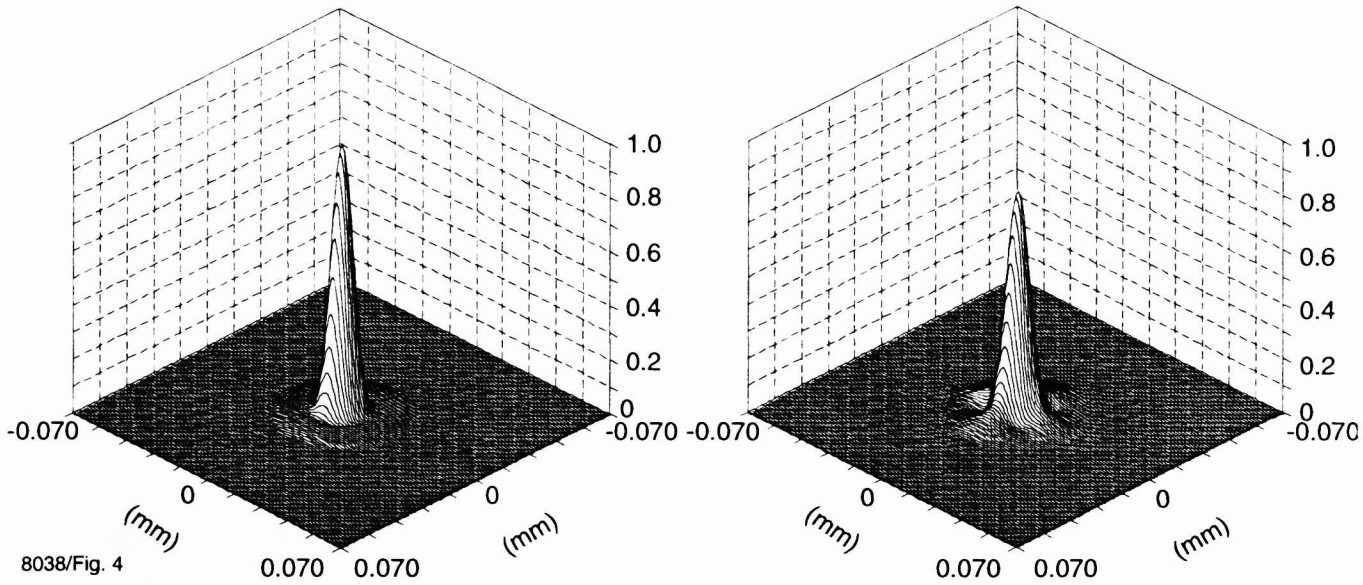

Figure 4. Polychromatic Diffraction Point Spread Functions (0.07 mm corresponds to 0.3 arcsec)

required lateral stability, while allowing the aluminum tube to expand and contract as the temperature changes. The metering rods maintain the separation between the mirrors.

Boron carbide has the best reflectivity of any known material in the 58- to 150-nm spectral region. An aluminum undercoating improves reflectivity in the 250- to 450-nm spectral region. The reflectivity of boron carbide on aluminum, measured at Goddard Space Flight Center (GSFC) is shown in Figure 5. Mirror coating would be done at GSFC.

6. STRAY LIGHT CONTROL

Stray light arises from two sources: (1) primary scatter from the primary and secondary mirrors due to residual roughness and possibly contamination and (2) secondary scatter, out-of-field light reaching the focal plane due to scatter from the inside of the telescope. Since SSO will carry out observations of faint sources in the presence of a bright object (for example, the Saturn magnetosphere with the bright planet only 40 arcsec away), we have established a requirement of 5–10 Å surface roughness for the mirrors.

Baffles, field stops, and a Lyot stop for suppression of out-of-field stray light from primary and secondary scatter are shown on Figures 6 and 7. A field stop is placed at the focus of the primary mirror, and second stop is placed in the hole in the center of the primary mirror. The Lyot stop is placed at the exit pupil for further suppression of stray light. Field and Lyot stops are part of the same structure. The field stop is a perforated four-sided pyramid having specular outside surfaces. It is supported on a four-legged spider assembly made of Invar. The legs of the spider assembly have a triangular cross section, with the sharp edge pointing towards the primary mirror. There are no direct illumination paths to the focal plane, and both primary and secondary scatter have been taken into account in designing the baffles.

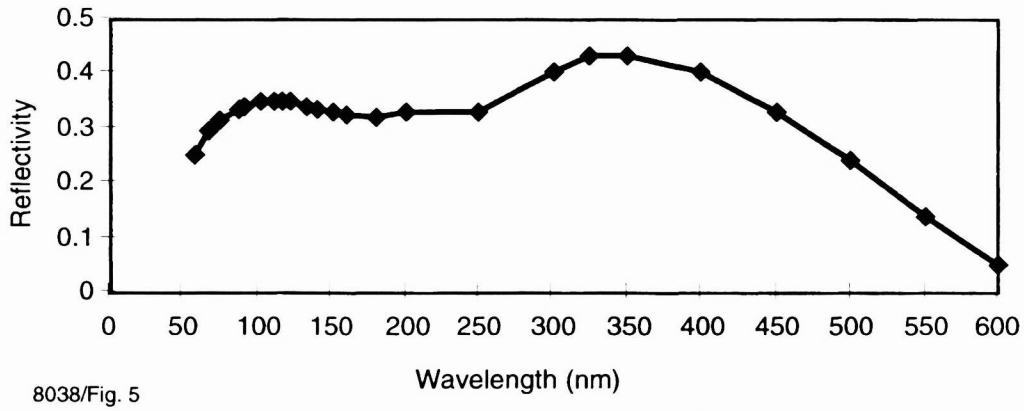

Figure 5. Measured Reflectivity of Boron Carbide Versus Wavelength

The baffle surfaces and the field and Lyot stops are made of bead-blasted aluminum for optimum efficiency in the ultraviolet. Most of the surfaces are diffuse, although some (such as the outside of the field stop assembly) will be specular to prevent secondary scatter from reaching the focal surface.

We used APART/PADE to calculate radiation scattered from the tube, mirrors, baffles, and struts to a spectrograph slit. The wavelength used was 308 nm, and a 10 cm autocorrelation length was assumed. We calculated the power deposited on a spectrograph slit having a dimension of 1 by 200 arcsec for various point-source angles measured with respect to the center of the slit. The calculations were made for a range of surface roughnesses, starting at 36 Å (the measured value for the HST primary mirror) and going down to 1 Å.

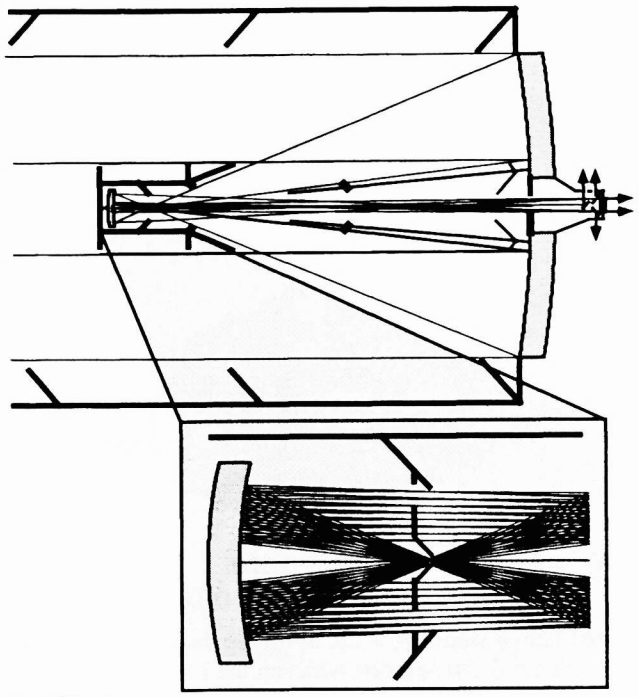

8038/Fig. 6

Figure 6. SSO Baffle Design

At small point-source angles, scattering from the primary mirror is the dominant factor. Figure 8 shows the point-source power at the spectrograph slit as a function of off-axis angle for surface roughnesses between 1 and 36 Å. The two top curves are for the HST with its measured 36 Å surface, and the SSO with an assumed 36 Å surface. Note that the SSO's Gregorian design already reduces stray light intensity by about 25:1 compared with the HST for the same mirror roughness, at off-axis angles up to about 1 arcmin. Reducing the SSO's surface roughness to 10 Å will reduce scattered power by about 350:1; and if the mirror surfaces can be polished to 5 Å, scattered power will be reduced by about 1400:1, compared with the HST. We have established 10 Å surfaces as requirements for SSO, with 5 Å surfaces as a goal.

With a 10 Å surface, scattered light from Saturn while imaging the magnetosphere would be undetectable, a marked improvement over the HST, where scattered light has the same intensity as the magnetosphere itself. We also calculated the scattered light count rate, with a 10 Å surface, with the Sun 7 deg from the optical axis. The count rate is only 2 counts per second, far below the count rate of a comet near perihelion. The combination of the Gregorian design and 10 Å mirror surfaces will permit observations never before performed.

The SSO mirror coatings have been designed for optimum reflectivity in the ultraviolet, but reflectivity in the visible and near infrared is very low (see Figure 5). This means that the mirror will have high emissivity, and will radiate an estimated 1000 W during observations against a deep space background. In addition, the mirror will absorb significant amounts of heat during operation near the direction to the Sun.

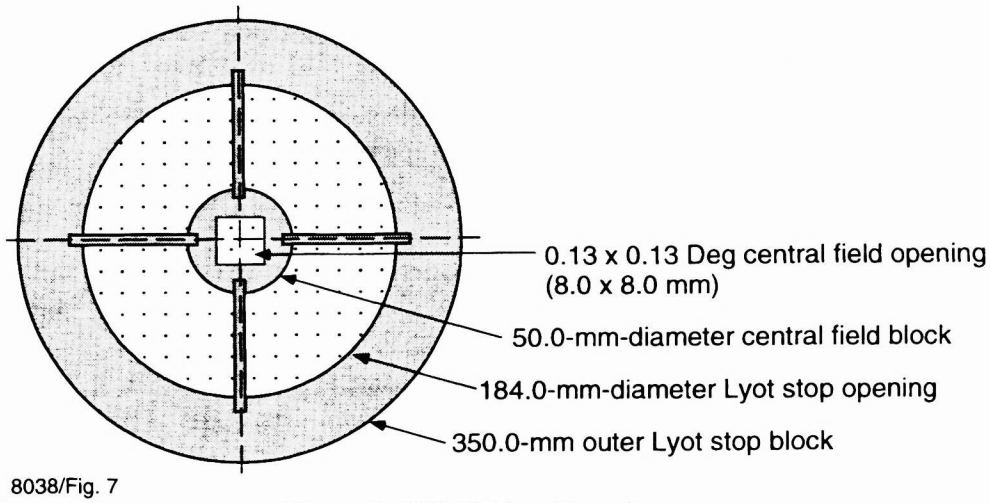

8038/Fig. 7

Figure 7. SSO Field and Lyot Stops

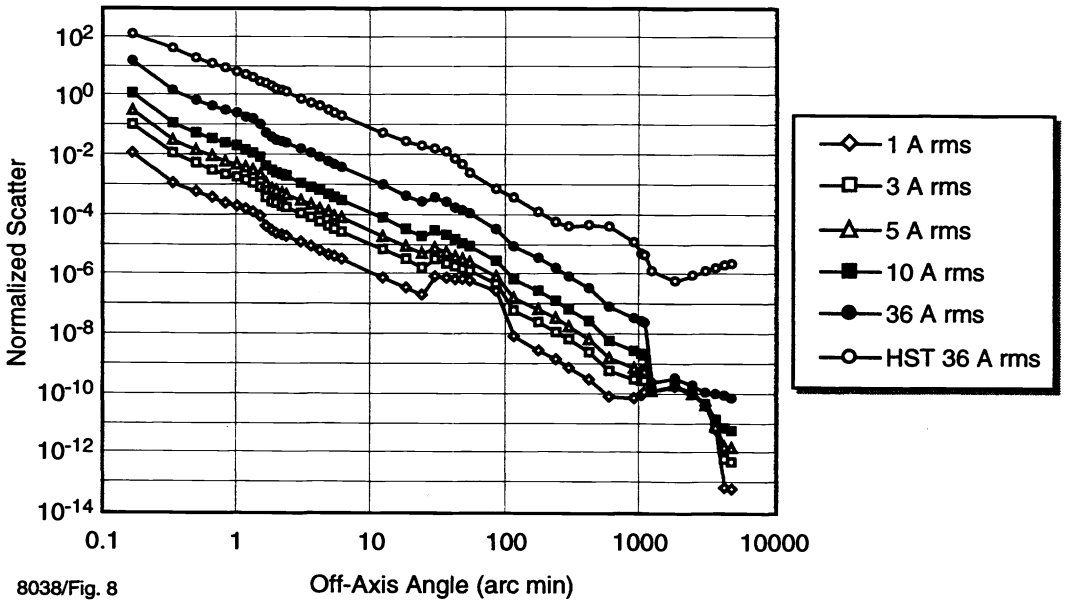

Figure 8. Stray Light Intensity Versus Off-Axis Angle and rms Surface Roughness

7. THERMAL CONTROL

The telescope is designed to remain in focus over wide temperature ranges, ± 10° C; however, a cold primary mirror will introduce unacceptable thermal gradients in the instrumentation section, and conversely, when observing near the Sun, will cause the instruments to heat up.

Our solution to these conditions is twofold: (1) incorporate active thermal control to hold the mirror at or near nominal temperature while observing against space, and (2) control the exposure time when observing toward the Sun. We believe that the limit on solar exposure will be driven by the temperature of the instruments, not the telescope.

Preliminary calculations indicate that, with the sun 7 deg from the optical axis, the rms wavefront error for SSO would be less than 0.1 wave rms for exposure times up to 2–3 minutes. Longer exposure times would be avoided when establishing comet observation profiles. A solar exposure would be followed by a heat dump to space, followed by a temperature equilibration period.

8. LINE-OF-SIGHT STABILIZATION

The LM-900 spacecraft will provide open-loop pointing to 10 arcsec, and a line-of-sight (LOS) stability of 0.2 arcsec, one sigma. However, the SSO will produce a polychromatic image in the UV 0.06 arcsec in diameter; and images will have to be stabilized to better than 0.2 arcsec on the spectrograph focal planes for optimum spatial and spectral resolution. Therefore, additional control of the LOS stability will be required, ideally to reduce the error residual to about 0.005 arcsec. This will be provided through the use of an inertial angle sensor (IAS), which is shown schematically in Figure 9.

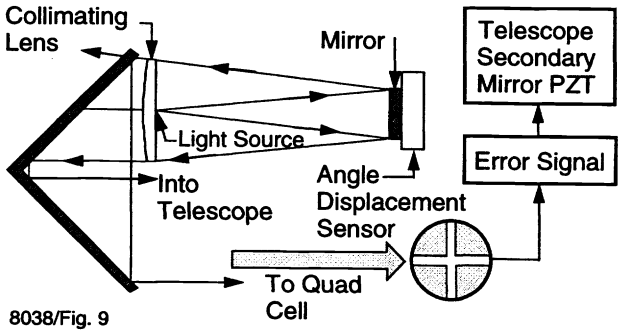

Figure 9. Schematic of Inertial Angle Sensor

A light source, typically a fiber fed by an LED, is placed at the second principal point of a lens having a diameter of 50 mm. Light emitted is reflected from a mirror placed one-half the focal length away. The mirror is articulated in tip-tilt via signals from an orthogonal pair of Systron & Donner 8301 angle displacement sensors (ADS), which are commercially available and space qualified; they are used on both HST and GOES.

Light emerging parallel from the IAS remains steady in inertial space and is injected into the telescope to provide a reference. The axis of the 50 mm beam is adjusted so that it makes its way to a quad cell installed in one corner of the focal plane. Any drift from the center of the quad cell will be due to spacecraft drift, or other factors. An error signal will be developed, and used to actuate the secondary mirror in tip-tilt, stabilizing the image. Designs of this type, sometimes called Inertial Pseudo Star Reference Units (IPSRU), have demonstrated LOS stability in inertial space to a few nanoradians, for angular deviations of up to about 10 arcsec.

This LOS stabilization method was developed for use on SDI, and several versions have been built and tested. The sensor whose performance is illustrated in Figure 10 was able to stabilize the line of sight in this laboratory demonstration to a maximum error of 24 nanoradians. This is approximately twice the SSO requirement.

9. OPTICAL TESTING

The end-to-end test configuration will be carried out using standard interferometric methods with a vertical optical axis using air-bag support for the primary mirror and a frequency-tripled YAG laser at 0.354-micron wavelength as a light source. We do not plan to perform an end-to-end resolution test, relying instead on the wavefront error measurements of the telescope assembly and normal optical alignment procedures.

The spectrographs will be calibrated by measuring throughput, comparing predicted signal levels with those actually observed.

10. SPACECRAFT

The SSO bus is a modified LM-900 spacecraft weighing 430 kg. Attitude control is via momentum exchange with four wheels providing stability of 0.2 arcsec (one sigma). Inertial reference is from an autonomous star tracker, with open loop pointing to 10 arcsec. Power is provided by a 150 amp-hr battery and three solar arrays. Command and data handling is from a radiation-hardened MIPS R3000 CPU with 4 to 8 Gbits of onboard memory. Communication is provided by a two-axis gimballed antenna. Active thermal control is provided by strip and zone heaters, and propulsion for wheel desaturation and orbit maintenance is via hydrazine thrusters. By utilizing a modified LM-900 spacecraft, we are able to capitalize on existing LM production and test facilities to provide a spacecraft bus at minimum cost and with very low risk.

Additional LOS stability beyond 0.2 arcsec will be provided via actuation of the telescope secondary mirror, using error signals derived from the IAS. Lockheed Martin has experience with articulated secondary mirrors for image stabilization, having employed the technique successfully on a number of programs, as well on SOHO and SPACELAB II. Use of a secondary mirror eliminates the need for an expensive attitude control system.

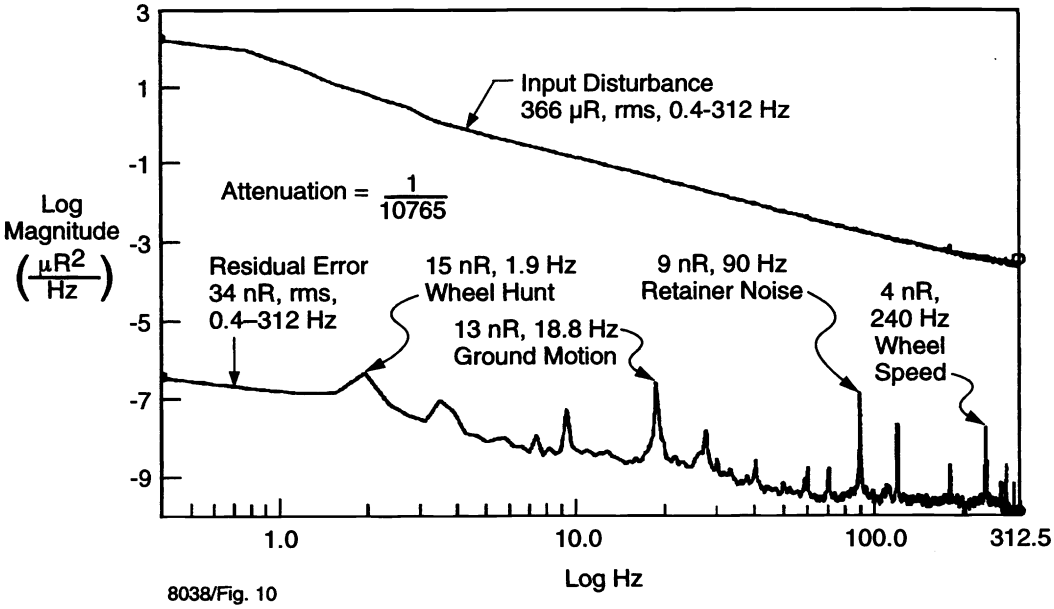

Figure 10. Measured Performance (Power Spectrum) of an Inertial Angle Sensor

The battery will satisfy power requirements during solar eclipse. The solar arrays will be oriented towards the sun during long observations, using a single-gimbal array adapted from LM's IRIDIUM® program. The arrays will be populated by GEO-qualified gallium arsenide solar cells from the LM A2100™ spacecraft. The gimbal will be locked during data collection to avoid disturbances.

11. WEIGHT ALLOCATION

Preliminary SST weight allocations are as follows:

Spacecraft Bus	430 kg
Telescope	650 kg
Instruments	65 kg
Total	1145 kg
Booster Throw Weight	1288 kg
Contingency	143 kg

12. GROUND STATION

The SSO ground station will be a turnkey installation provided by Scientific Atlanta (SA). SA is under contract to provide the ground stations for both the IRIDIUM® and CRSS programs. It includes a 5-m dish to be used for both transmit and receive operations, a 200-W S-band transmitter, an S-band receiver/demodulator, data recorders, data server, and joystick control of telescope pointing. The system may operate in either normal or safe mode. In safe mode, automatically activated commands will close the telescope door.

During normal operation, commands will be uplinked to the spacecraft in the 2025 to 2110 MHz band at 10 Kbps, and telemetry will be downlinked from the satellite in the 2200 to 2300 MHz band at 1 Mbps.

13. OPERATIONAL CONTROL

Telescope pointing will be provided by commands which will place the target near the center of the telescope's field of view. Fine guidance will be provided by a joystick for the operator to position the target in real time. Output from the slit jaw imagers (for joy stick pointing and correlation tracking), spectrographs, and broadband imager will be routed to the existing data processing subsystem, a MIPS R-3000 radiation-hardened CPU addressing an onboard high-speed storage unit (HSSU). The HSSU has a design storage capacity up to 80 Gbits. We will install 4 to 8 Gbits, depending on weight, power, and cost. Data are sent to the signal-conditioning electronics, and then to the high-gain communication system.

Short-term ground data storage will be provided by a local data server that may be accessed through the Internet. Long-term data storage will be provided through either tape backup or CD-ROM.

14. REFERENCES

1. P.D. Feldman, "Ultraviolet Spectroscopy and the Composition of Cometary Ice," *Science* **219**, p. 347, 1983.
2. J.C. Green, W. Cash, T.A. Cook, and S.A. Stern, "The Spectrum of Comet Austin from 910 to 1190 A," *Science* **251**, p. 408, 1991.
3. M.F. A'Hearn, R.L. Millis, D.G. Schleicher, D.J. Osip, and P.V. Birch, "Ensemble Properties of Comets: Results from Narrow-Band Photometry of 85 Comets, 1976-1992," *Icarus* **118**, p. 223, 1995.
4. D.E. Shemansky, "Energy Branching in the Io Plasma Torus: The Failure of Neutral Cloud Theory," *J. Geophys. Res.* **93**, p. 1773, 1988.
5. F. Bagenal, "Empirical Model of the Io Plasma Torus: I. Voyager Measurements," *J. Geophys. Res.* **99**, p. 11043, 1994.
6. D.E. Shemansky and D.T. Hall, "The Distribution of Atomic Hydrogen in the Magnetosphere of Saturn," *J. Geophys. Res.* **97**, p. 4143, 1992.
7. D.E. Shemansky, P. Matheson, D.T. Hall, H.-Y. Hu and M. Tripp, "Detection of the Hydroxyl Radical in the Saturn Magnetosphere," *Nature* **363**, p. 329, 1993.
8. A. Seiff et al. "Structure of the Atmosphere of Jupiter: Galileo Probe Measurements," *Science* **272**, p. 844, 1996.

9. C.L. Emerich et al. "Evidence for Supersonic Turbulence in the Upper Atmosphere of Jupiter," *Science* **273**, p. 1085, 1996.

10. B. Haisch and J. Schmitt, "Advances in Solar Stellar Astrophysics," *Publ. Astr. Soc. Pacific* **108**, pp. 113-129, 1996.

11. T. R. Ayres et al. "Redshifts of High-Temperature Emission Lines in the Far-ultraviolet Spectra of Late-Type Stars," *Ap. J.* **274**, pp. 801-814, 1983.

12. H. Achour, P. Brekke, O. Kjeldseth-Moe, and P. Maltby, "Observed Redshifts in the Solar Transition Region above Active and Quiet Regions" *Ap. J.* **453**, p. 945, 1995.

13. S. Baliunas and R. Jastrow, "Evidence for long-term brightness changes of solar-type stars," *Nature* **348**, pp. 520-523, 1990.

APPENDIX A PRESCRIPTION FOR THE SSO TELESCOPE

```
LENS
LI,SSO 2.4 Meter Gregorian with Stops & Masks 28 Feb 98
WV .35 .3 .4 .25 .45
SAY 1200
SCY FANG .067 -3.7419876219084
C, SURFACE NO. 0
TH 1.7E+26
AIR
C, SURFACE NO. 1
ID, dummy
COBS 300
TH 3200
AIR
C, SURFACE NO. 2
ID,primary mirr
CC -.99949053
REFS
CV -1.8115942028986E-4
CLAP 1200
COBS 200
PY
REFL 0 222
C, SURFACE NO. 3
ID,field stop
CLAP 25
COBS RECT -4 4
TH -217.18819
AIR
C, SURFACE NO. 4
ID,secondary
CC -.799806
PUY .025
CLAP 110
PCY
REFL 0 -51
C, SURFACE NO. 5
ID,exit pupil
CLAP 175
COBS -92
TH 2756.5916
AIR
C, SURFACE NO. 6
ID,primary hole
CLAP 200
COBS RECT -70 70
TH 800
AIR
C, SURFACE NO. 7
ID,image
CV .00460817
CLAP RECT 60 60
EOS
PM LENO 14
UNITS MM
C ..... END OF LENS DECK .....
```